Adaptive 3D Gamut Mapping Based on Color Distribution of Image

Ryoichi Saito and Hiroaki Kotera
Department of Information and Image Sciences, Chiba University
Chiba, Japan

Abstract

Gamut Mapping between display and print images is a most typical application. Current gamut mapping algorithm (GMA) is mostly addressed to compress the out-of-gamut colors into the inside of printer gamut. Indeed, the highly saturated gamut images such as CG images on monitor are necessary to be compressed to make the appearance matching to print. However, the printer gamut has been much expanded with the improvements in printing media and devices. Hence, source image doesn't always fill the entire device gamut, and sometimes its' gamut need to be enlarged to get the better color renditions. This paper proposes an advanced GMA designed to work dependent on the image color distributions. The proposed GMA includes two types of mappings, one for compression and other for expansion of the image gamut. A quick decision whether image is compressed or expanded, is decided using both printer and image gamut.

Introduction

The proposed system selects the compression GMA or extension GMA whether the image gamut is obviously larger or extremely smaller than printer gamut. Figure 1 shows how a CG image gamut is larger and a natural scene gamut is smaller than the inkjet printer gamut. Figure 2 illustrates the process diagram of the proposed GMA. In the compression GMA, the source colors are mapped into the inside of printer gamut based on the image-to-device 3D gamut boundary relations. We proposed a method for comparing the gamut between image and device, where the device and image color distributions are divided into small segments by discrete polar angle. There, the maximum radial vectors for image and device are extracted and compared in each segment. The gamut shell is described as the simple radial distances, named *r-image*. The key point in this compression GMA is to use the relations in only two vectors in each divided segment. While in the extension GMA, the image gamut is stretched to the Gaussian distribution function as a target in lightness and chroma histograms. The extension GMA is aimed to preferred color reproduction.

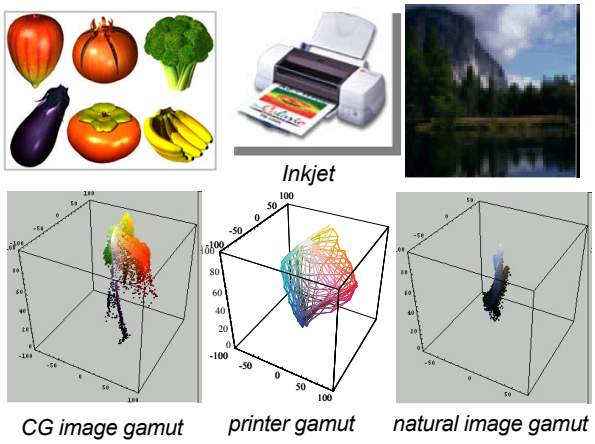

Figure 1. Two types of image vs. device gamut relations

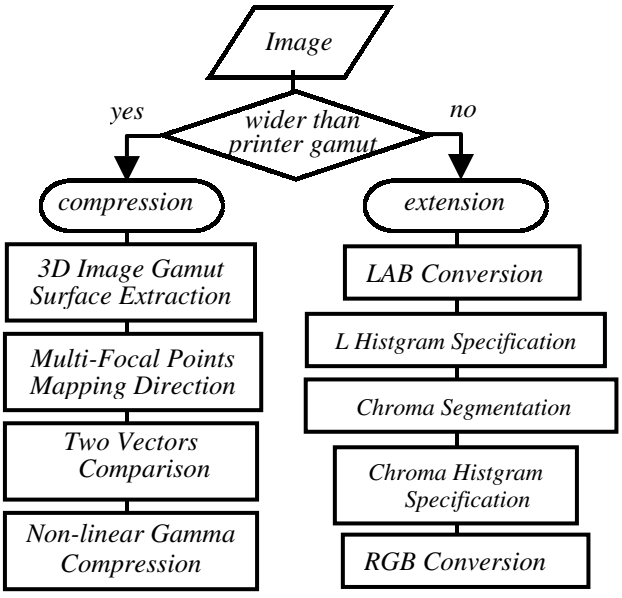

Figure 2. Diagram of proposed gamut mapping system

3D Gamut Compression

Image-to-Device Mapping

In the current 2D ***D-D*** GMA,[1,2] the source color *s* is mapped to the destination *t* in relation to the monitor gamut boundary vs. printer's boundary toward a focal point ***p***. However, the saturation and gradation losses will happen after the mapping, because the image color distributions don't always fill the entire monitor gamut. While, the ***I-D*** GMA[3,4,5,9] uses the image gamut boundary ***i***, then it can suppress such losses in minimum (See Fig. 3).

Since the 2D mapping is done in a hue segmented Lightness-Chroma (L-C) plane, the unwanted artifacts often appear when passing across the one hue leaf to another. Here we extended the 2D I-D into seamless 3D I-D GMA[3].

The key points to success in 3D GMA are

- Extraction of 3D image Gamut Surface & Description
- Use of Non-linear Mapping Function
- Mapping into Multi-Focal Points depending on lightness distribution

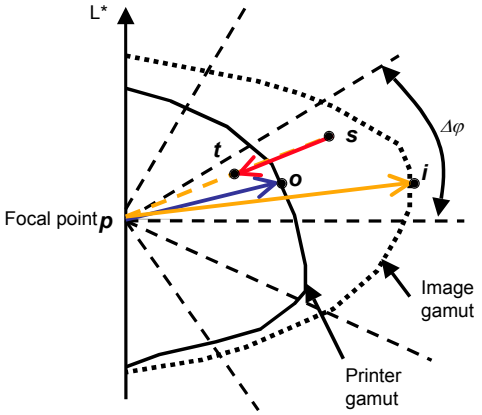

Figure 3. Basic Concept of I-D (Image-to-Device) GMA in 2D

Extraction of 3D Image Gamut Surface

We have developed an automatic gamut surface extract-ion algorithm[8] from a random color distribution as shown in Fig. 4. The random color distributions of source image in the CIELAB space are segmented by a constant polar angle step, that is, $\Delta\theta$ in hue angle and $\Delta\phi$ in sector angle between a color vector and the lightness axis. In general, the image color center $[L^*_0,a^*_0,b^*_0]$ should be defined as a gravity center. However, to perform GMA, the center must be placed at the same point for both printer and images. Here the center was set at a neutral point $[L^*_0,a^*_0,b^*_0] = [50,0,0]$.

$$\theta = \tan^{-1}\left(\frac{b^*-b^*_{avg}}{a^*-a^*_{avg}}\right) \quad (1)$$

$$\phi = \tan^{-1}\left(\frac{L^*-L^*_{avg}}{\left[(a^*-a^*_{avg})^2+(b^*-b^*_{avg})^2\right]^{1/2}}\right) \quad (2)$$

We define the radial matrix $\boldsymbol{r}_{gamut}$ whose element is given by the maximum radial vector in each polar angle segment.[8] The image gamut is described by the radial matrix $\boldsymbol{r}_{gamut}$ (See Fig. 4).

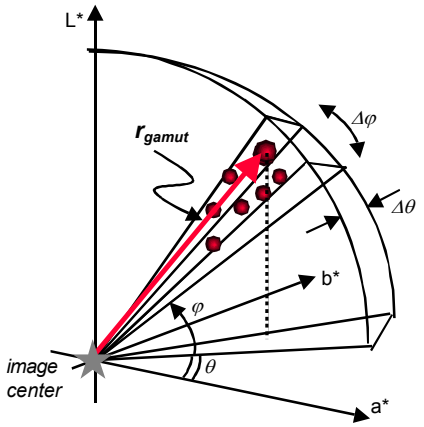

Figure 4. 3D Gamut surface extraction method

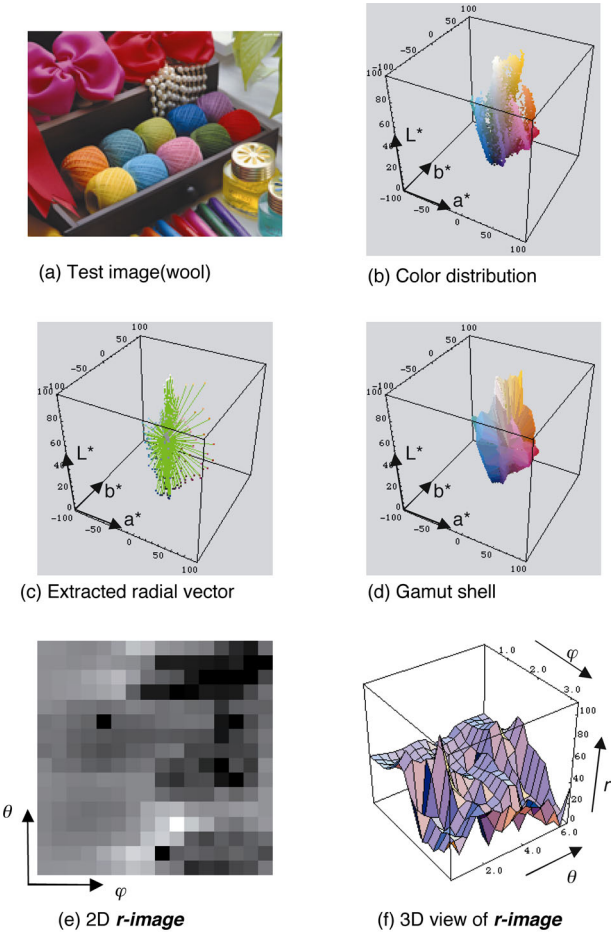

Figure 5. Gamut surface of "wool"

Definition of *r-image*

Figure 5(a) and (b) show the sRGB test image "wool" and its color map in CIELAB. The extracted maximum

radial vectors are shown in Fig. 5(c), and (d) is its gamut shell rendered by connecting these radial vectors. We proposed to replace the 3D radial vectors 2D distance array arranged in rectangular lattice point (j,k), named *r-image*. Figure 5(e) shows the *r-image* represented as a 2D gray scale image segmented in 16 ×16 discrete angles. Figure 5(f) shows its 3D representation in Cartesian coordinates. A gamut volume is intelligibly visualized in this 3D view.

Nonlinear Gamma Compression Function

In 3D CIELAB space, a source color ***s*** is mapped to target ***t*** along the mapping line toward focal point ***p*** referencing to the image gamut boundary ***i*** and output device gamut boundary ***o*** as given by the following vector notations.

$$\overrightarrow{pt} = \overrightarrow{po} \cdot \left(\frac{\overrightarrow{ps}}{\overrightarrow{pi}} \right)^{\gamma} \tag{3}$$

Here, γ represents the gamma-compression coefficient.

The GMA works as linear compression for γ=1, and as nonlinear compression for 0<γ<1.

Mapping Towards Multi-Focal Points

In the design of GMA, the mapping direction to a focal point is very important. To keep the natural lightness, a mapping into the multi-focal points is desirable. We took the control parameters, $\boldsymbol{p}_{lower}$ and $\boldsymbol{p}_{upper}$ into account to setting the multi-focal points.[9] Here $\boldsymbol{p}_{lower}$ and $\boldsymbol{p}_{upper}$ are placed at the minimum and the maximum L^* points where the gamut boundary slope is changed from high to low and low to high respectively. Image and printer lightness are divided by polar angles under $\boldsymbol{p}_{lower}$ and over $\boldsymbol{p}_{upper}$, and by the parallel segments between $\boldsymbol{p}_{lower}$ and $\boldsymbol{p}_{upper}$. Figure 6(b) shows the overview of the multi-focal point method with two convergent lightness points of $\boldsymbol{p}_{lower}$ and $\boldsymbol{p}_{upper}$. In the ink-jet printer used in this experiment, $\boldsymbol{p}_{lower}$ and $\boldsymbol{p}_{upper}$ were set to $[L^*_0, a^*_0, b^*_0]$= [58, 0, 0] and $[L^*_0, a^*_0, b^*_0]$=[45, 0, 0].

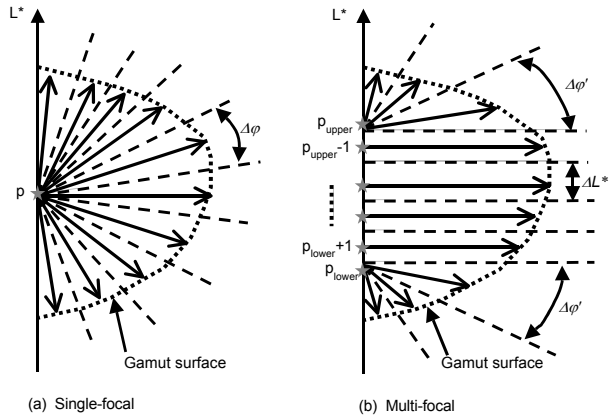

*Figure 6. Decision of multi-focal points by **ILD** method*

3D Gamut Compression Result

A psychophysical experiment has been carried out to compare the color appearance matching between the original CRT image and the printed image after mapping. Three kinds of test images, one CG image and two sRGB images were used for this experiment. In our ***I-D GMA*** experiments, the three different mapping conditions were set to (1): single-focal with gamma-compression coefficient γ=0.8, (2): multi-focal with γ=0.8, (3): multi-focal with γ=0.5. The proposed ***I-D GMA*** was compared with (5): ***D-D GMA*** and (4): the ***Clipping GMA***. Both were also performed in 3D divided segment. Figure 7 shows the evaluation results for test images. In every picture, ***D-D GMA*** obviously showed the worst result. The result clearly shows that the mapping to the multi-focal points generally give the better image appearances. In case of the image "wool", however, ***Clipping GMA*** got the better score. The selection of GMA types with optimal mapping parameters is dependent of image contents and fully automatic process is left for future works.

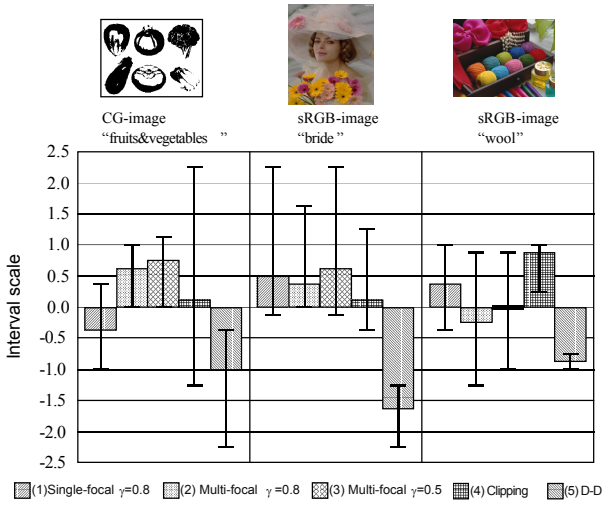

Figure 7. Evaluation Result of Psychophysical Experimet.

Gamut Extension for De-saturated Image

Objectives of Image Gamut Extension

The major objective of gamut extension is to recover the degraded colors taken under insufficient illumination or faded colors after long preservation. It is difficult to restore the lost original colors exactly, but possible to recover the pleasant colors by gamut extension. Sometimes, the pictures even if taken by digital camera, only fill the narrow gamut ranges as compared with modern wide gamut media such as hi-fi inkjet print and hoped to be corrected to vivid colors.

Gamut Extension by Color Histogram Specification

We proposed an image gamut extension method based on Histogram Specification (HS).[6,7] To simplify the process, the histograms of luminance and chrominance are extended separately in CIELAB space as the following steps.

(1) RGB to LAB conversion
(2) Gaussian HS for L component
(3) Segmentation of chroma component
(4) Gaussian HS for chroma component

Gaussian Histogram Specification for Y image

Histogram Equalization (HE) method is useful to expand the reduced dynamic ranges of monochrome image. However, HE can't be applied to tri-color images, because it causes unnatural and unbalanced color appearance. There is no definitive solution to what shapes of the color histogram are comfortable. In our experiments, Gaussian histogram was an effective candidate to create the natural and pleasant images. First, the histogram of lightness L is converted to the Gaussian distribution through HE as follows.

The original lightness L is transformed to g by HE and the histogram $p_1(L)$ is flattened to constant $p_c(g)$ as

$$g = F(L) = \int_0^Y p_1(x)dx, \quad p_c(g) = \textbf{constant} \tag{4}$$

where, $p_1(L)$ denotes the probability density of value L occurrence. Now, our target histogram $p_2(z)$ is Gaussian

$$p_2(z) = \frac{1}{\sqrt{2\pi}\sigma}\exp\left\{-\frac{1}{2\sigma^2}(z-\bar{z})^2\right\} \tag{5}$$

and z is also equalized into constant $p(g)$ by HE as

$$g = G(z) = \int_0^z p_2(x)dx, \quad p_c(g) = \text{constant} \tag{6}$$

Thus, connecting two g's after HE from L to g and z to g, the objective transform from L *to* z is given by the inverse

$$z = G^{-1}(g) = G^{-1}(F(L)) \tag{10}$$

Gaussian Histogram Specification for Chroma Image

After the histogram specification of L, the chrominance components are segmented into m divisions by ΔH in hue angle H. Then chroma C of each division is extended by Gaussian HS as same as L without changing color hue. For example, whole pixels are segmented into totally m = 16 divisions and each was extended by individual Gaussian HS.

Considerations on Neutral Gray and Multiple Peaks

Furthermore, the achromatic areas were excluded beforehand from the process to avoid the unwanted coloring of grayish pixels. Sometimes, the L histogram has not always a single peak but multiple peaks. For such cases, the histogram was specified to multiple Gaussian distribution functions centered at peak positions in original L histogram.

Figure 8 shows an improved image by gamut extension using Gaussian histogram specification. The lightness L histogram was specified to multiple Gaussian distribution functions and naturally stretched to wide range. The chroma was segmented to 16 ΔH division and each division was also extended by Gaussian HS algorithm. The picture taken in dim light was dramatically improved to comfortable image with the bright and vivid colors.

Conclusion

The paper proposed an approach to GMA from both sides of compression and extension. Two different GMAs were introduced, one for compression from wide to narrow and the other for extension from narrow to wide gamut. We could design the 3D compression GMA logically, but have no definitive design rule for the extension GMA at present. However both algorithms are based on the common concept of "***image-dependent***". Future works will be continued to find the better gamut extension algorithm based on this concept and on the human visual appearance tests.

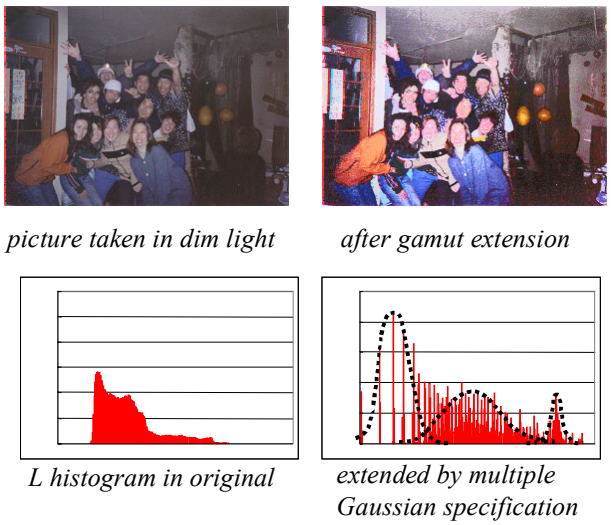

Figure 8. Improved image by gamut extension

References

1. J. Morovic and M. R. Luo, *Col. Res. Appl.* 26,pp.85-102 (2001).
2. L. W. MacDonald and M. R. Luo, *Color Imaging,* John Wiley & Sons (1999).
3. H. S. Chen and H. Kotera, *JIST*, 46, pp.44-631 (2002).
4. R. Saito and H. Kotera, *Proc. IS&T's 17th NIP*, pp.454-457 (2001).
5. R. Saito and H. Kotera, *Proc. ICIS'02, TOKYO*, pp.407-408 (2002).
6. H. Kotera, et al, *Proc. PICS Conf. '01*, pp. 288-292 (2001).
7. H. Kotera, et al, *Proc. AIC Color '01*, pp. 227-228 (2001).
8. H. Kotera and R. Saito, *Proc. 9th IS&T/SID CIC*, pp.56-61 (2001).
9. R. Saito and H. Kotera, *Proc. IS&T's 18th NIP*, pp.608-611 (2002).

Biography

Ryoichi Saito received his BS degree in Image Science from Chiba University in 1983. Since 1983, he has been working on direct plate making, digital image processing and color reproduction at Chiba University.